Bulk Biopolyelectrolyte Complexes from Homopolypeptides:

Solid "Salt Bridges"

Zachary A. Digby, Yuhui Chen, Khalil Akkaoui, Joseph B. Schlenoff*

Department of Chemistry and Biochemistry

The Florida State University, Tallahassee, FL 32306-4390, United States

Abstract

Salt bridges, pairings between oppositely-charged amino acids, are dispersed throughout proteins to assist folding and interactions. Biopolyelectrolyte complexes (BioPECs) were made between the homopolypeptides poly-*L*-arginine (PLR) and poly-*L*-lysine (PLK) with sodium triphosphate (STPP), as well as from polypeptide-only combinations. Viscoelastic measurements on these high salt bridge density materials showed many were solid, even glassy, in nature. Although the polypeptide-phosphate complexes had similar moduli at room temperature, the PLR-STPP complex displayed an unusual melting event above 70 °C not seen in PLK-STPP. This event was supported with differential scanning calorimetry. Infrared spectroscopy showed the PLK-STPP system contained β-sheets while PLR-STPP did not. Stoichiometric, macroscopic BioPECs of PLR and PLK with poly-*L*-aspartic acid (PLD) and poly-*L*-glutamic acid (PLE) were made. PLR-PLD was found to undergo a melting event similar to that in PLR-STPP. ATR-FTIR studies showed that BioPECs made with PLD do not contain β-sheets, while those comprised of PLE do.

This work illustrates an expanded palette of unique properties from these biomaterials, such as strong viscoelastic differences between PECs containing PLE and PLD, even though they differ by only one carbon on the side chain.

Introduction

(Bio)polymer "coacervation," the spontaneous separation of homogenous solutions of polymers into two or more distinct phases, has been a research focus for nearly a century after initial reports by Bungenberg de Jong and Kruyt.¹ This liquid-liquid phase separation (LLPS) into a polymer rich phase and polymer poor phase has been proposed as a potential mechanism for the formation of membraneless organelles.²⁻⁵ While the systems are not completely understood, they have been shown to be important in regulatory systems within living cells.⁶ Biomolecules have been shown to be catalytically active within these organelles, forming a locus for reactions.⁷⁻⁹ It was recently reported that it is possible to form these coacervates between short-chain peptides and ATP, which then entraps and regulates the activity of the protein cytochrome c.¹⁰

Coacervation may occur between biological (macro)molecules or between synthetic systems with similar underlying science.

11-15 Interactions between opposite charges feature prominently among the many intermolecular interactions providing a driving force for coacervation. Synthetic polyelectrolytes form liquid-like or solid-like coacervates or complexes (both termed "PECs"). The materials properties of synthetic systems depend on variables such as the charged functional group, salt type/concentration, and pH.

18-19 These variables allow tunability of the material properties and potential transitions between solid-like and liquid-like complexes, and on to complete dissolution of the PEC.

complexation is thought to be primarily the gain in translational entropy from counterion release.²⁰⁻²¹ Under certain circumstances complexation is reversed by adding a salt. Typically, the systems that are most easily dissolved by salt have an endothermic enthalpy of complexation.¹⁸ Biological PECs are more often liquid-like, which leads to a droplet morphology during (micro)phase separation.

Pairings between oppositely-charged amino acids in proteins are known as "salt bridges," ²² thought to enhance the stability of the folded state. A common method to quantify the stabilization is by comparing the energy of unfolding of the wild-type protein to that of a mutated protein that has undergone a point mutation to remove the amino acid(s) responsible for the salt bridge. ²³ Salt bridges are complex and depend on the location within the protein, as some salt bridges may decrease stability. ²⁴ A biomaterial formed between polypeptides in which every repeat unit is charged represents the highest density of salt bridges.

In more biologically-based systems, LLPS with biomacromolecules such as DNA and RNA are focused on gene regulation and protein interactions. ²⁵⁻²⁶ Bridging the gap between biological systems and synthetic systems are synthetic biopolymers made from peptide repeat units. ²⁷⁻²⁸ Recent works also probe the fundamentals of LLPS, such as investigating salt effects. ²⁹ Some work has taken a more materials-like approach and investigated the thermoresponsive properties of these materials, ³⁰⁻³¹ as well as applications such as drug delivery. ³² Peptide-based materials tend to form secondary structures such as α -helixes and β -sheets found in proteins. ^{19, 27-28, 33-40} Materials with more solid-like properties have been observed with certain systems. ^{4, 27, 41} Early work focused on complexes between DNA and copolymers of L-alanine and L-lysine, resulting in B-type DNA patterns superimposed on an α -helix. ⁴² Moving away from DNA and RNA, mixed systems with one homopolypeptide, such as poly-L-glutamic acid, complexed with

oligo(ethyleneimine)s have been investigated. This work suggested a critical chain length of 6 repeat units was needed (on at least one polyelectrolyte) to form secondary structures 19 – a requirement that depended on the system. Based on the literature, if secondary structures are to be formed, one may assume that at least twenty repeat units are sufficient to do so. $^{40-41, 43-44}$

A charge of ± 4 on the complementary (poly)ion species in the complex is the minimum number of charges needed to distort secondary structure/formation. ¹⁹ This critical charge was shown to be important in synthetic systems, leading to a large increase in the viscoelastic modulus of the material. ¹¹ Biologically relevant small molecules such as nucleosides (i.e. adenosines and uridines) have also been investigated. It was shown that ATP (4 charges) will form a coacervate with a short peptide containing 4 cationic residues, while AMP (2 charges) will not. ¹⁰ Similarly, ADP (3 charges) is unable to complex with poly-L-lysine (under physiological conditions) and hydrolysis of ATP to ADP results in droplet dissolution. ⁴⁵⁻⁴⁶ Poly-L-lysine or poly-L-arginine with more than 10 repeat units were able to form a coacervate with ADP and ATP. ⁴¹ Arginine-based polymers have stronger interactions than lysine-based polymers due to π - π interactions via the guanidinium group. ⁴⁷⁻⁴⁸ The stronger interactions of arginine resulted in coacervates with a 100-fold increase in viscosity compared to those made with polylysine. ⁴⁹

Scheme 1. Structures of poly-*L*-lysine (PLK), poly-*L*-arginine (PLR), poly-*L*-aspartic acid (PLD), poly-*L*-glutamic acid (PLE), and sodium triphosphate pentabasic (STPP). All counterions are omitted for clarity.

Chirality effects on secondary structures of homopolypeptide-based PECs have been a focal point for investigation. One of the most notable works used a polyglutamic acid/polylysine system. Perry et al. concluded that PECs comprised of homochiral homopolypeptides (D with D, L with L, or D with L), resulted in β -sheet formation. PECs containing β -sheets formed solid-like PECs while PECs comprised of one racemic homopolypeptide resulted in liquid-like PECs containing no β -sheets. Similar results have been seen in other studies on the same system. Switching poly-L-glutamic acid with poly-L-aspartic acid (complexed with poly-L-lysine) results in a PEC with no β -sheets. Most of the literature on homopolypeptide PECs focuses on polylysine as the polycation and polyglutamic acid as the polyanion. Only a few works have

evaluated polyarginine-based PECs,⁴⁰⁻⁴¹ viscoelastic properties,⁵⁰ and temperature effects³⁵ on homopolypeptide blends.

The purpose of the present work is twofold: first, PECs between polycations poly-L-lysine (PLK) or poly-L-arginine (PLR) with a small inorganic phosphate molecule (sodium triphosphate pentabasic, STPP) are probed for secondary structures and viscoelastic properties. STPP, a common inorganic biophosphate, is structurally similar to the phosphate tail of ATP but lacks the nucleoside head-group. Second, the secondary structures and viscoelastic properties of polyarginine PECs are compared to those of polylysine PECs. When complexed with STPP, PLR systems have higher viscoelastic moduli but lack the β -sheets observed in PLK systems that provide thermal stability. PECs between homopolypeptides reveal that polyaspartic acid (PLD) systems lack β -sheets while polyglutamic acid (PLE) systems contain β -sheets. Structures of polypeptides used and STPP can be found in Scheme 1. All systems that contain β -sheets have thermal stability but do not result in an overall higher viscoelastic modulus.

Experimental Section

Materials

Poly-*L*-arginine hydrochloride (PLR, molecular weight, MW, 38,500), poly-*L*-lysine hydrochloride (PLK, MW 66,000), and poly-*L*-aspartic acid sodium salt (PLD, MW 27,000) were from Alamanda Polymers. Sodium triphosphate pentabasic, NaCl, sodium azide, 3-(N-morpholino)propanesulfonic acid (MOPS), and poly-*L*-glutamic acid sodium salt (PLE) (MW, 84,600) were from Sigma-Aldrich. Deionized water (18 M Ω cm) (Barnstead, Nanopure) was used to prepare all solutions. Isotopic sodium chloride (22 NaCl, 54 μ Ci, >99% purity) was from Perkin Elmer and potassium thiocyanate (KS 14 CN, 100 μ Ci, > 99% purity) was from ViTrax.

Phosphate-polypeptide and Polypeptide-polypeptide Complexes

Poly-*L*-arginine, poly-*L*-lysine, poly-*L*-aspartic acid, poly-*L*-glutamic acid, and sodium triphosphate pentabasic were vacuum-dried at room temperature for 24 h before transfer to an Arfilled glove box to be weighed. 0.125 M polypeptide solutions in 0.15 M NaCl, 20 mM MOPS buffer, and 200 ppm of sodium azide (as a preservative) were mixed with either equal volumes of phosphate salt solutions at molar concentrations resulting in stoichiometric charge ratios, or equal volumes of the oppositely charged polypeptide solution. The resulting PECs were then vortexed for 10 min and centrifuged for 4 h at 12,000 rpm. The supernatant was removed from the centrifuge tube (except for the PLK-PLD complex that resulted in a liquid PEC, which was left in the centrifuge tube and later had the solution replaced). PECs were partially dried under vac for 6 h. The PECs were placed into a stainless steel 8 mm diameter mold and pressed at room temperature for 24 h. The PEC tablets were then removed from the mold and placed into a 20 mL vial filled with aqueous 0.15 M NaCl, 20 mM MOPS (pH 7), and 200 ppm of sodium azide to equilibrate for 24 h.

Rheology

Measurements of linear viscoelastic response (LVR) were performed using a strain-controlled rheometer (DHR-3 TA Instruments) with Peltier temperature control. An 8 mm parallel plate geometry was used throughout. A custom-designed lower plate had a reservoir for buffer with a cap to prevent evaporation (see Supporting Information Figure S1). Prior to loading, all PECs were soaked in 0.15 M NaCl, 20 mM pH 7 MOPS buffer and 200 ppm sodium azide for 24 h, which was also added to the solution reservoir to maintain a pH-controlled aqueous environment for the PECs. The PECs were first transferred onto the upper plate. The upper plate was then lowered onto the lower plate until a force of 0.1 N was achieved. Modulus as a function of

temperature from 0 to 90 °C was determined at 1 Hz with a ramp rate of 2 °C min⁻¹, with the exception of the PLK-PLE system, which was only heated to 40 °C.

Attenuated Total Reflectance-Fourier Transform Infrared Spectroscopy (ATR-FTIR)

ATR-FTIR spectra were collected using a ThermoScientific Nicolet iS20 with a Specac Heated Golden Gate ATR attachment equipped with a diamond crystal. The temperature of the ATR was calibrated with a Fluke thermocouple. All PECs were soaked in D₂O for a total of 48 h, with a change in D₂O after 24 h to remove any residual H₂O. The PECs were placed on the thermal stage with excess D₂O and a circular anvil with a sealing O-ring compressed the samples onto the crystal. The temperature controller was set to 25 °C and the sample was allowed to equilibrate at temperature for 5 min prior to spectra collection. High temperature spectra were taken immediately after without release of the anvil, letting the samples equilibrate for 5 min at 85 °C. The same procedure was used for concentrated single components (STPP or polypeptide) dissolved in D₂O.

Differential Scanning Calorimetry (DSC)

A TA Q1000 DSC was used to determine the melting temperature, if one existed, of PLK-STPP and PLR-STPP. PEC powder was dried at 120 °C for 24 h and stored under Ar until it was loaded into a Tzero aluminum pan (TA Instruments) in a dry box. Hydrated PEC samples were prepared by combining a known amount of dry PEC with a known amount of water prior to hermetically sealing the pan and allowing a 24 h hydration period. For hydrated samples, the first two heat-cool ramps were done at a rate of 20 °C min⁻¹ from 20 °C to 90 °C to remove any thermal history. The third heat-cool ramp was done at a rate of 10 °C min⁻¹ with the same temperature range. The same procedure was used for dry samples, with a temperature range of 30 °C to 170 °C. All samples were maintained under N₂ and the third heating ramp was used to determine any

transitions.

Water Content

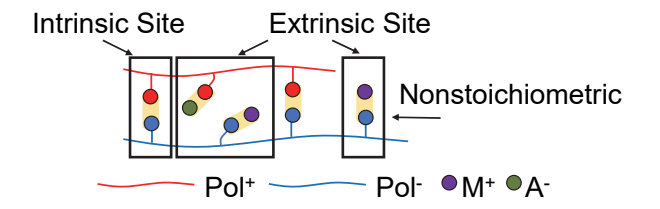
To determine the water content of the PECs, stoichiometric PECs were hydrated for 24 h in buffer solution. The PECs were then dabbed dry and weighed. Following weighing, they were placed in an oven at 120 °C overnight to dry. The dry weights were recorded and subtracted from the hydrated weight to find the weight of water in each PEC.

¹H NMR

¹H solution NMR experiments (Avance 400 MHz, Bruker) were conducted to determine isotopic impurities in PLD and PLE. PLD and PLE powders were dissolved in D₂O at a concentration of 10 mg mL⁻¹.

Radiolabeling

To maintain net electroneutrality, all charged units that are not paired with an oppositely-charged unit must be paired with a counterion. Replacing these counterions with radiolabeled ions provides an accurate and sensitive method of determining the ion population within a PEC. Scheme 2 depicts counterions introduced by doping in concentrated salt solutions and counterions that are always required to balance nonstoichiometric polyelectrolyte charges. Exposure of PECs to dilute (e.g. 1 mM) solutions of ions produces only the latter.



Scheme 2. Illustration of intrinsic sites (polycation paired with polyanion) and extrinsic sites

(polyelectrolytes paired with oppositely charged counterions, due to doping and nonstoichiometry) within a PEC.

Radiolabeled NaSCN was used as a salt to exchange and label counterions within PECs. 22 Na $^{+}$ is available as 22 NaCl and S 14 CN $^{-}$ is available as KS 14 CN. 22 Na-labeled NaCl (γ -emitter, half-life = 2.62 years, $E_{max} = 511$ keV, activity: 54 μ Ci mL $^{-1}$ stock solution) was used to prepare a 1 μ Ci solution of 1.0 mM 22 NaSCN (specific activity: 0.1 Ci mol $^{-1}$) by adding 20 μ L of 22 NaCl stock solution to 10 mL 1.0 mM NaSCN. 14 C-labeled KSCN (β emitter, half-life = 5730 years, $E_{max} = 158$ keV, specific activity: stock solution 100 μ Ci mL $^{-1}$, ViTrax) was used to prepare a 2 μ Ci solution of 1.0 mM NaSCN. (specific activity: 0.2 Ci mol $^{-1}$) by adding 20 μ L of KS 14 CN stock to 10 mL 1.0 mM NaSCN. PECs were soaked for 18 h in each salt solution to allow enough time for the system to reach equilibrium, or for radioactive isotope to self-exchange with their non-radioactive counterparts.

To account for the excess polyanion, the PECs were first soaked in 10mL 1.0 mM NaSCN followed by 10 mL 1.0 mM 22 NaSCN. The radioactive solution was removed, and PEC transferred into a plastic scintillation vial and placed on plastic scintillator (6 mm thickness and 38 mm diameter, SCSN-81 Kuraray). The counts were recorded using an RCA 8850 photomultiplier tube (PMT) powered at -2300 V and connected to a frequency counter (Philips PM6654C) with a 10 s gate time and -20 mV pulse threshold. 100 μ L of the 1.0 mM 22 NaSCN was added to the scintillation vial as a standard.

To account for excess polycation, anions in PECs exchanged by rinsing in NaS¹⁴CN (1.0 mM). The PEC was then dabbed dry. The S¹⁴CN⁻ ions labeling extrinsic polycations sites were extracted from the complex using 2 mL 1.0 mM NaSCN and a 100 μL aliquot of this was mixed with 2 mL salt-tolerant liquid scintillating cocktail (EcoLume, ICN). The counts were then

measured using a Charm II 6600 System (Charm Sciences) using the 14 C channel. 100 μ L of the 1.0 mM NaS 14 CN was added to the scintillation cocktail as a standard.

Results and Discussion

Both small molecules and polypeptides with opposite charges were used to prepare complex coacervates with homopolypeptides. A stoichiometric combination of charges under the conditions used was verified with sensitive radioisotopic labeling techniques. Though having much in common in terms of composition, the physical properties of these complexes spanned a wide range of morphologies and responses to temperature. Solid-like PECs were pressed into macroscopic shapes (discs) which enabled the measurement of classical bulk viscoelastic responses. Previous work has probed the viscoelastic response of PECs comprised of PLK or PLR with STPP, however temperature sweeps were not reported. ¹¹ Though viscoelastic responses for liquid-like PECs have been reported for mixed chirality systems, ⁵⁰ to our knowledge, viscoelastic responses for solid-like PECs of homopolypeptide combinations have not been reported.

Phosphate-Polypeptide Complexes

FTIR (in the ATR mode) is typically used to determine the presence of secondary structures in polypeptide-containing complexes such as coacervates and "multilayer" ultrathin films. Absorptions assigned to α-helix formation occur at 1635 or 1650 cm⁻¹ and β-sheets yield absorptions at 1610 cm⁻¹ and a low intensity absorption near 1680 cm⁻¹.^{27-28, 33-34} Because H₂O absorbs at 1643 cm⁻¹, samples were hydrated with D₂O, giving an absorption at 1209 cm⁻¹, out of the secondary structure sensitive region.³³ ATR-FTIR spectra of concentrated solutions of individual PEC components are shown in Figure S2. STPP features do not appear in the sensitive region (1600-1700 cm⁻¹) as shown in Figure S2A. Solution PLK displays one absorption near 1640

cm⁻¹ in Figure S2B, which indicates a random confirmation.³³ PLR displays multiple absorptions at 1670 and 1640 cm⁻¹ (Figure S2C). These absorptions correspond to turns and random confirmation, with no defining secondary structure. Both homopolypeptides undergo little change upon heating from 25 to 85 °C, indicating that the transition event observed below in rheology and DSC for the PLR-STPP complex is not due to *inherent* secondary structures (or secondary structure changes) of the individual peptides.

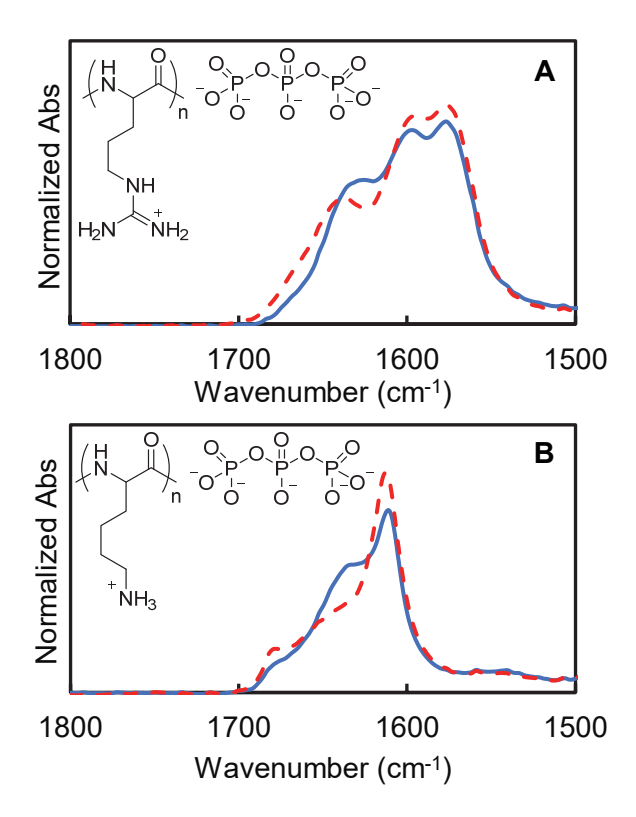


Figure 1. ATR-FTIR spectra for areas of interest of (A) PLR-STPP in D₂O, blue solid line, 25 °C; red dashed line, 85 °C; (B) PLK-STPP in D₂O, blue solid line, 25 °C; red dashed line, 85 °C. The inset shows structures of the homopolypeptides and sodium triphosphate.

The PLR-STPP complex does not have β -sheets as seen in Figure 1A, but does have α -helix absorptions at 1635 cm⁻¹. Interestingly, this absorption does not decrease as significantly with temperature as it does in the PLK-STPP complex. PLR is known to form α -helixes upon

binding to other molecules and plays an important role in tunneling through cellular membranes.⁵¹ The IR spectra of PLK-STPP complex shown in Figure 1B and S1A, exhibit characteristic β -sheet absorptions at 1610 and 1680 cm⁻¹. These absorptions are present at both 25 and 85 °C. There is a shoulder at 1635 cm⁻¹ indicating the presence of α -helixes as well, but the absorption decreases from 25 to 85 °C, suggesting a loss of α -helix structure that the β -sheets do not experience.

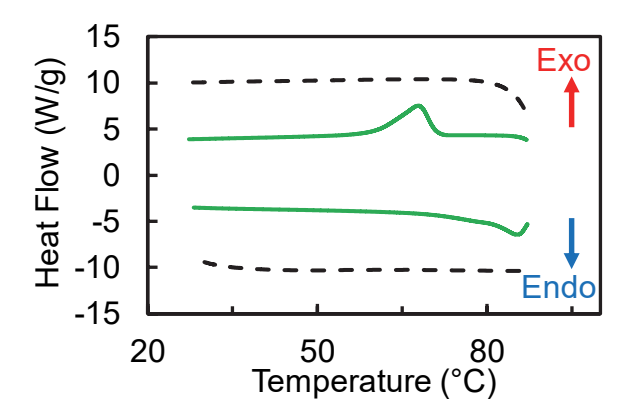


Figure 2. Differential scanning calorimetry thermograms of hydrated PLR-STPP complex (green solid line) and hydrated PLK-STPP complex (black dashed line). All curves shown are from the third heating/cooling cycle at a ramp rate of 10 °C min⁻¹. Peaks for the heating (lower) and cooling (upper) curves of PLR-STPP are found at 85 and 68 °C respectively. All curves have been shifted vertically to avoid overlap.

To probe the changes in secondary structures, differential scanning calorimetry (DSC) was performed. DSC of the hydrated PLR-STPP complex in Figure 2 shows an event occurring at 85 and 68 °C in the heating and cooling ramps, respectively. This event resembles a phase transition rather than a glass transition (Tg). The PLK-STPP complex shows no thermal events (Figure 2) despite having a larger change in the ATR-FTIR spectra. DSC was also performed on dry PECs and dry individual polymers. Figure S4A shows that in the dry PLR-STPP complex, the event does not occur, suggesting water is required. From DSC of dry PLR, a Tg of 110 °C was observed

(Figure S4B). Due to the large shift in T_g expected upon hydration of PLR, it is most likely below 0 °C. Therefore, it is not observed in the rheology or DSC data in any of the PEC systems. DSC of dry PLK-STPP and PLK (Figures S4C and S4D), showed no significant event and no observable T_g for PLK.

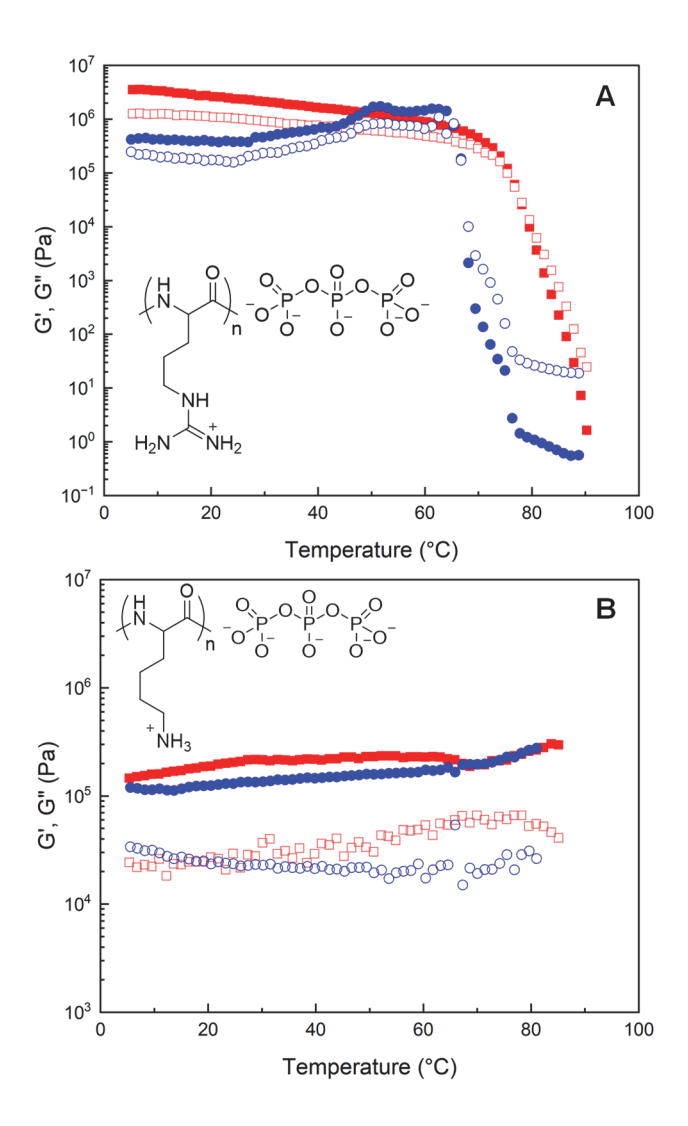


Figure 3. Linear viscoelastic response for (A) PLR-STPP and (B) PLK-STPP. The samples were immersed in 0.15 M NaCl for 24 h at a pH of 7, and the temperature sweep was performed from 0 to 90 °C, then back to 0 °C and a temperature ramp rate of 2 °C min⁻¹. Storage modulus G' and

loss modulus G" were recorded at 0.1 Hz using a strain verified to be in the linear viscoelastic region. Both the third heating (red squares; G' filled symbols and G" open symbols) and cooling (blue circles, G' filled symbols and G" open symbols) ramps are shown.

Figure 3 shows the linear viscoelastic properties of both the PLR-STPP complex (A) and PLK-STPP complex (B) fully hydrated in 0.15 M NaCl pH 7 (i.e. close to physiological conditions) as a function of temperature. The frequency sweeps for these systems have been published previously. The PLR-STPP complex shown in Figure 3A displays unusual behavior when heated above ~70 °C. The severe drop in moduli, not previously observed, indicates that the PEC goes from a solid-like material to a liquid-like material. This melting is reversible in the sense that the modulus is recovered on cooling and returns to its starting point of about 4 x 10⁶ Pa after time at low temperature. The hysteresis in modulus versus temperature, not a result of thermal lag of the apparatus, is probably due to kinetic limitations of internal reorganization/solidification, which is also thought to be the cause of the maximum in G' and G" at about 60 °C seen in Figure 3A.

This reversible event does not occur in the PLK-STPP complex, as shown in Figure 3B, which is solid-like from 0-90 °C. The transition temperatures in rheology are close to the temperatures seen in the heating and cooling curves of the DSC data (Figure 2). Multiple samples and multiple scans of the PLR-STPP complex were used to confirm that the event was reproducible. On heating above the transition temperature, the material goes from opaque and hard to clear and viscous. On cooling, the PEC becomes opaque and stiffens into its current shape. The opacity is taken as indirect evidence of internal microphase separations within the PEC, which is common for glass-forming PECs. 52-53

Polypeptide-Polypeptide Complexes

PECs of PLR-PLD and PLK-PLD do not contain significant amounts of β -sheets at room temperature (Figure 4A and 4C). Both show characteristic α -helix absorptions at 1635 cm⁻¹. PLR-PLE and PLK-PLE, in contrast, exhibit characteristic β -sheet absorptions at 1610 and 1680 cm⁻¹. In these systems it appears that the polyanion has more influence over the secondary structure formation as both PLE systems form β -sheets while the PLD systems do not.

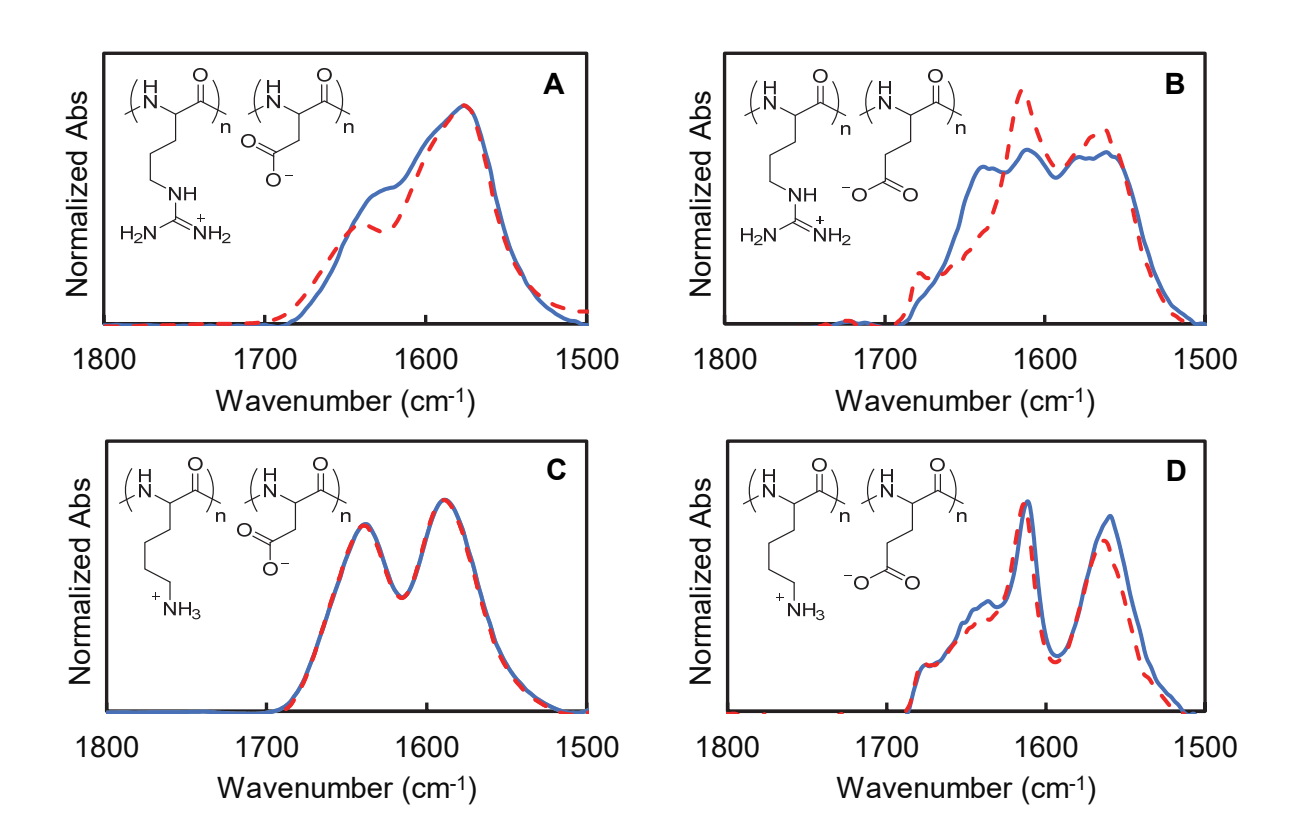


Figure 4. ATR-FTIR spectra for areas of interest of (A) PLR-PLD, (B) PLR-PLE, (C) PLK-PLD, and (D) PLK-PLE. All PECs were soaked in a D₂O solution; blue solid line is for 25 °C; red dashed line is for 85 °C (C only went up to 45 °C). All spectra are normalized to the C-N stretching peak at 1400 cm⁻¹ (extended wavenumber axis provided in Figure S4).

Heating the PECs in an identical fashion to the STPP complexes in Figure 1, results in

changes in some PECs while others undergo virtually no change. On heating PLR-PLD there is a decrease in the absorption at 1625 cm⁻¹ which is attributed to α -helixes. PLR-PLE shows β -sheet absorptions at 1610 and 1680 cm⁻¹ that increase upon heating, similar to PLK-STPP. There is a small increase in the water content of the PEC as seen by the intensity increase of the water absorption in Figure S5. The water content appears to be unchanged in the PLR-PLD system.

PLK-PLD formed a coacervate and was already liquid-like at room temperature, therefore the temperature was only mildly increased to 45 °C. There were virtually no changes observed between the lower and elevated temperatures. PLK-PLE shows β -sheet absorptions at 1610 and 1680 cm⁻¹ similar to PLR-PLE, however for the PLK system there is not an increase in the β -sheet absorptions at elevated temperature. There is a similar increase in water content in Figure S4. Comparing these four systems, it appears that PLE is the main contributor to β -sheets, or rather that PLD may be the reason for lack of β -sheets.

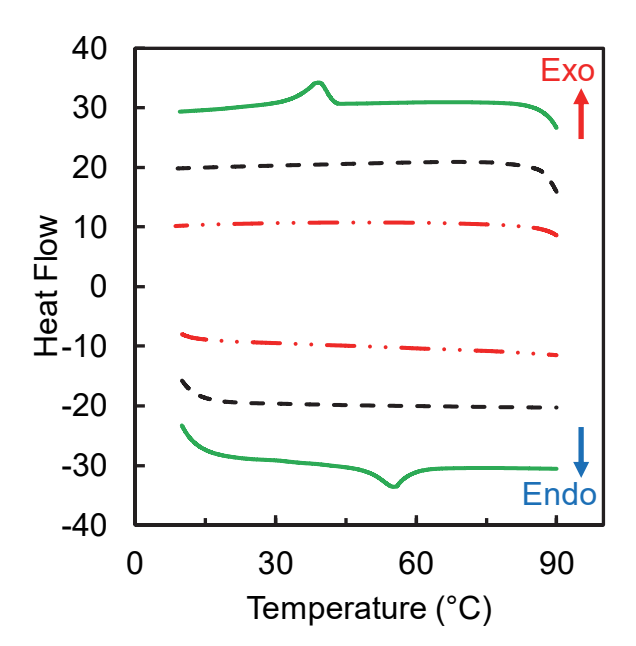


Figure 5. Differential scanning calorimetry thermograms of hydrated PLR-PLD (green solid line), hydrated PLR-PLE (red dashed and dotted line), and hydrated PLK-PLE (dashed black line). All

curves shown are from the third heating/cooling cycle at a ramp rate of 10 °C min⁻¹. Peaks for the heating (bottom green) and cooling (top green) curves of PLR-PLD are found at 56 and 41 °C respectively. All curves have been shifted to avoid overlap.

Similar to the STPP systems, DSC was used to identify thermal transitions in the peptide-peptide systems. Figure 5A shows an event at 56 and 41 °C in the heating and cooling ramps, respectively, of the PLR-PLD PEC. The IR data in Figure 4A shows a drop in the α-helix content upon heating, which may be associated with the events seen here. Figures 5B & 5C both are flat and do not show any changes. This suggests that the increase in β-sheets, as well as the increase in water content, shown for the PLR-PLE in Figures 4B and S4 do not result in a transition or any measurable heat flow. The same can be said for the PLK-PLE water content increase. The water content for the PECs at room temperature can be found in Table S2.

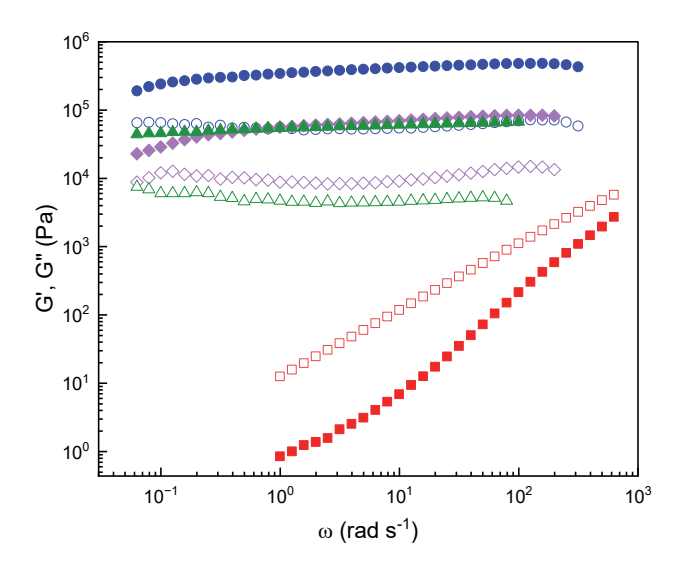


Figure 6. G' and G" versus frequency for PLR-PLD (purple diamonds), PLR-PLE (blue circles), PLK-PLD (red squares), and PLK-PLE (green triangles). Storage modulus G' (filled symbols) and loss modulus G" (open symbols) are shown as a function of frequency. All samples were run under

physiological conditions (37 °C, 0.15 M NaCl, 20 mM pH 7 MOPS).

Frequency sweeps for the peptide-peptide systems under physiological conditions are shown in Figure 6. The PLR-PLE system has the highest storage and loss modulus of the polypeptide-polypeptide PECs, followed by PLR-PLD and PLK-PLE respectively. PLK-PLD, has much lower moduli which is expected of liquid-like PEC. It was unexpected that PLR-STPP has the highest modulus even though one of the components is a small molecule.

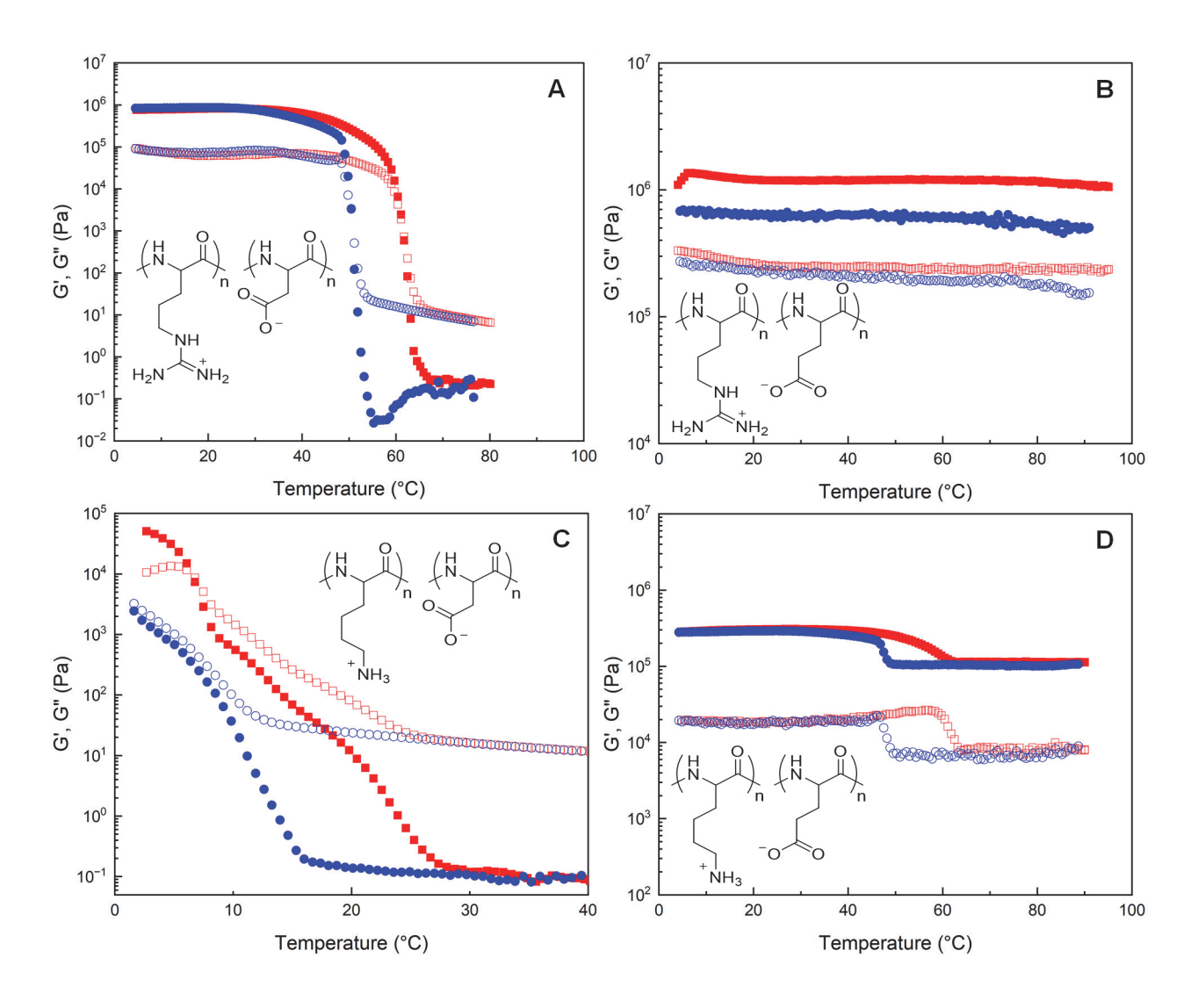


Figure 7. Linear viscoelastic response at 0.1 Hz for (A) PLR-PLD, (B) PLR-PLE, (C) PLK-PLD,

and (D) PLK-PLE. Samples were soaked in 0.15 M NaCl for 24 h at a pH of 7 and the temperature sweep was performed from 0 to 90 °C (except for C, which was 0 to 40 °C) and then back to 0 °C at a temperature ramp rate of 2 °C min⁻¹. The third heating (red squares, G' is filled and G" is open) and cooling (blue circles, G' is filled and G" is open) ramps are shown.

The viscoelastic response to temperature sweeps for polypeptide combinations are all unique. Figure 7A for PLR-PLD undergoes a similar melt transition to that seen in Figure 3A for the PLR-STPP complex. Similarly, this event is also evident in the DSC thermogram in Figure 5A. Figure 7B maintains PLR as the polycation, while switching PLD to PLE (addition of one CH₂ in the R group). This small structural change results in a linear viscoelastic response that *lacks* the transition event seen in Figure 7A, and instead has minor rheological response to temperature change, typical for a glass. The ATR-FTIR data in Figure 4B shows an increase in β-sheet content, an effect which would presumably increase the moduli at elevated temperatures. This is likely compensated by the increase in water content seen in Figure S4B, resulting in a nearly constant modulus over the temperature range investigated.

Switching the polycation to PLK, when paired with PLD as seen in Figure 7C results in a liquid-like PEC. G' flattens out after 30 °C because the torque has fallen below the limit of instrument sensitivity.⁵⁴ PLK-PLE yields a slight drop in the moduli above 50 °C, but this is not a transition similar to PLR-PLD as there is no corresponding feature discernable in the DSC (Figure 4C). The drop is likely due to an increase in the water content, seen in Figure S4D, but it is *not* balanced by an increase in β-sheet content, unlike PLR-PLE. Previous work by Boulmedais et al. suggested for PLK-PLE systems that there was a possible amide formation at high temperature (89 °C) between the carboxylic acid group of PLE and the amine of PLK.³⁵ That is not the case here as PLK-PLD would have crosslinked, losing its liquid-like properties. Previous

studies on thermal crosslinking of polyacrylic acid/polyallylamine multilayers were performed using temperatures of at least 130 °C for 2 h, which are far from the conditions in this work.⁵⁵ The melting events seen in PLR-STPP and PLR-PLD are similar to reversible thermal denaturation events (protein unfolding) seen in some proteins.⁵⁶⁻⁵⁸ Reversible denaturation does not always disrupt secondary structures within a protein, but does disrupt higher ordered structures.⁵⁹

Some discrepancy exists within the literature regarding the secondary structure of the PLK-PLD system. In their earlier works, Schaaf and co-workers suggested that PLK-PLD does not form β -sheets. ³⁵⁻³⁶ Follow-up work from Pilbat et al. suggested that PLK-PLD does form β -sheets, but lacks the characteristic absorptions near 1610 and 1680 cm⁻¹. ³⁴ Instead the band from 1637-1638 cm⁻¹ was assigned as "a low-frequency component of the extended chains, that is, β -structures" following previous studies on proteins. ⁶⁰ These works primarily investigated polyelectrolyte multilayers of polypeptides. Cakmak et al. investigated "bulk" coacervates and found no β -sheet formation, agreeing with the work presented here. ⁴¹ Perry et al. indirectly supports the absence β -sheets, as their work in "bulk" systems found β -sheets resulted in solid precipitates, which are not seen by Cakmak et al. or this work. ²⁷

One possible explanation for the discrepancy may be due to the stoichiometry of the PECs. Polycation and polyanion incorporation during the buildup of a polyelectrolyte multilayer are not always equal,⁶¹ and may result in non-stoichiometric PECs, which alter the material properties.⁶² The polypeptide-polypeptide complexes presented here were radiolabeled and identified to be almost stoichiometric (see Table S1). Further studies investigating the effects of stoichiometry on secondary structures of both "bulk" PECs and polyelectrolyte multilayers may be fruitful. Another possible explanation comes from the work of Itoh et al., which suggests that multilayer buildup using polypeptides goes through a unique mechanism in which the β-sheet structures are produced

at the interface as a result of charge compensation between polyelectrolytes within the multilayer.³⁷ The β -sheets then act as nuclei for further propagation, which is different than "bulk" complexation by mixing equimolar solutions of polycation and polyanion. Therefore, secondary structure formation may be influenced by the method of complexation.

In "bulk" PECs, it is unclear why PLD systems appear to not contain β-sheets while PLE systems do. Hydrophobic interactions between side chains are thought to play a role in β-sheet stabilization. 63-64 Due to the smaller sidechain in PLD, these stabilizing hydrophobic effects could be too weak. Furthermore, complexes with PLD and PLE have been investigated with the positively charged bone morphogenetic protein 2 (BMP-2) as potential regenerative bone therapies. It was found that PLE was drastically superior to PLD in modulating the activity of BMP-2. Activities within cells were not correlated with the properties of polymers such as the molecular weight or pKa, and it was concluded that the chemical structure of PLE is more suitable to form a complex. While no investigation of secondary structure was performed, this suggests that a small difference in the hydrophobic section of the polymer results in large interaction differences.

Quan et al. have demonstrated that commercially available PLD can be both enantiomerically and isomerically impure. They found that PLD₁₀₀ from Alamanda Polymers was only 80% L, and 20% D. Perry et al. have demonstrated how important chirality is for secondary structure formation, therefore it is possible that the lack of secondary structure in PLD systems shown here is due to enantiomer impurities. PLD can be connected by either α -peptide linkages (desired) or β -peptide linkages (enantiomer impurity). PLD₁₀₀ was found to be 29:71 (% α :% β) by Quan et al. by ¹H NMR. In the work presented here, PLD₂₀₀ was found to be 20:80 (% α :% β) as shown in Figure S5. The increase in flexibility of the backbone may result in lack of

 β -sheets. PLE, both in the literature 66 and this work, was found to be almost 100% pure.

Conclusion

Solid-like, in addition to liquid-like, PECs incorporating homopolypeptides represent an interesting class of biomaterials. Secondary structures and viscoelastic properties of PECs between PLK and PLR with STPP and between all-peptide complexes illustrated a range of internal structure (or lack of it) and viscoelastic properties. It was found that in the phosphate systems, PLR-STPP does not have β -sheets while PLK-STPP does. It is thought the β -sheets in the PLK-STPP system provide thermal stability, shown by the lack of melt transition in the β -sheetless PLR-STPP PEC. However, PLR-STPP has a modulus one order of magnitude higher than PLK-STPP, suggesting that β -sheets are not a dominating factor in viscoelastic properties.

Similarly for the PECs comprising all homopolypeptides, those that contain β -sheets (PLR-PLE & PLK-PLE) have thermal stability. It is unclear why PECs from PLD lack β -sheets while those from PLE contain them. Comparing the homopolypeptide PECs, PLR-PLE has the highest modulus at 4 x 10⁵ Pa, which is only slightly higher than PLR-PLD and PLK-PLE which are roughly identical. PLK-PLD has the lowest modulus as it is the only liquid-like polypeptide PEC under physiological conditions. These findings illustrate the wide range of materials properties of polypeptide PECs and include a melting-like transition not previously reported. The addition of chirality (e.g. L/L vs. L/D vs. racemic) to variables would no doubt expand the range of responses and properties even further.

Acknowledgments

Funding: This work was supported by a grant from the National Science Foundation DMR -

10.1021/acs.biomac.2c01456

2103703.

Author Information

Corresponding Author

* Email: jschlenoff@fsu.edu

ORCID

Zachary A. Digby: 0000-0001-5018-9620

Yuhui Chen: 0000-0002-5416-2350

Joseph B. Schlenoff: 0000-0001-5588-1253

Notes

The authors declare no competing financial interest.

Data and materials availability

All data are available in the manuscript or supplementary materials.

Supporting Information

Determination of polypeptide/polypeptide PEC stoichiometry; ATR-FTIR of solutions; ATR-FTIR of STPP complexes; DSC of dry materials; ATR-FTIR of peptide-peptide

complexes; water content of PECs; ¹H NMR of polyanions

References

1. Bungenberg de Jong, H. G.; Kruyt, H. R., Coacervation (Partial Miscibility in Colloid Systems). *Proc. Koninkl. Med. Akad. Wetershap.* **1929**, *32*, 849-856.

2. Hyman, A. A.; Weber, C. A.; Jülicher, F., Liquid-Liquid Phase Separation in Biology. *Annu. Rev. Cell Dev. Biol* **2014**, *30*, 39-58.

- 3. Booij, H. L.; Bungenberg de Jong, H. G., Colloid Systems. In *Biocolloids and their Interactions*, Springer Vienna: Vienna, 1956; pp 8-14.
- 4. Abbas, M.; Lipiński, W. P.; Wang, J.; Spruijt, E., Peptide-Based Coacervates as Biomimetic Protocells. *Chem. Soc. Rev.* **2021**, *50*, 3690-3705.
- 5. Aumiller, W. M.; Keating, C. D., Experimental Models for Dynamic Compartmentalization of Biomolecules in Liquid Organelles: Reversible Formation and Partitioning in Aqueous Biphasic Systems. *Adv. Colloid Interface Sci.* **2017**, *239*, 75-87.
- 6. Berchtold, D.; Battich, N.; Pelkmans, L., A Systems-Level Study Reveals Regulators of Membraneless Organelles in Human Cells. *Mol. Cell* **2018**, *72*, 1035-1049.e5.
- 7. Holehouse, A. S.; Pappu, R. V., Functional Implications of Intracellular Phase Transitions. *Biochemistry* **2018**, *57*, 2415-2423.
- 8. Boeynaems, S.; Holehouse, A. S.; Weinhardt, V.; Kovacs, D.; Van Lindt, J.; Larabell, C.; Van Den Bosch, L.; Das, R.; Tompa, P. S.; Pappu, R. V.; Gitler, A. D., Spontaneous Driving Forces Give Rise to Protein-RNA Condensates with Coexisting Phases and Complex Material Properties. *Proc. Natl. Acad. Sci. U. S. A.* **2019**, *116*, 7889-7898.
- 9. Ukmar-Godec, T.; Hutten, S.; Grieshop, M. P.; Rezaei-Ghaleh, N.; Cima-Omori, M.-S.; Biernat, J.; Mandelkow, E.; Söding, J.; Dormann, D.; Zweckstetter, M., Lysine/RNA-Interactions Drive and Regulate Biomolecular Condensation. *Nat. Commun.* **2019**, *10*, 2909.
- 10. Saha, B.; Chatterjee, A.; Reja, A.; Das, D., Condensates of Short Peptides and ATP for the Temporal Regulation of Cytochrome c Activity. *Chem. Commun.* **2019**, *55*, 14194-14197.
- 11. Yang, M.; Digby, Z. A.; Chen, Y.; Schlenoff, J. B., Valence-Induced Jumps in Coacervate Properties. *Sci. Adv.* **2022**, *8*, eabm4783.
- 12. Wang, Q.; Schlenoff, J. B., The Polyelectrolyte Complex/Coacervate Continuum. *Macromolecules* **2014**, *47*, 3108-3116.
- 13. Li, L.; Srivastava, S.; Andreev, M.; Marciel, A. B.; de Pablo, J. J.; Tirrell, M. V., Phase Behavior and Salt Partitioning in Polyelectrolyte Complex Coacervates. *Macromolecules* **2018**, *51*, 2988-2995.
- 14. Spruijt, E.; Cohen Stuart, M. A.; van der Gucht, J., Linear Viscoelasticity of Polyelectrolyte Complex Coacervates. *Macromolecules* **2013**, *46*, 1633-1641.
- 15. Tsuchida, E., Formation of Polyelectrolyte Complexes and Their Structures. *J. Macromol. Sci. A* **1994,** *31*, 1-15.
- 16. Fu, J.; Fares, H. M.; Schlenoff, J. B., Ion-Pairing Strength in Polyelectrolyte Complexes. *Macromolecules* **2017**, *50*, 1066-1074.
- 17. Schlenoff, J. B.; Yang, M.; Digby, Z. A.; Wang, Q., Ion Content of Polyelectrolyte Complex Coacervates and the Donnan Equilibrium. *Macromolecules* **2019**, *52*, 9149-9159.
- 18. Digby, Z. A.; Yang, M.; Lteif, S.; Schlenoff, J. B., Salt Resistance as a Measure of the Strength of Polyelectrolyte Complexation. *Macromolecules* **2022**, *55*, 978-988.
- 19. Abe, K.; Koide, M.; Tsuchida, E., Complexes of Poly(L-glutamic acid) with Oligo(ethyleneimine)s and their Quaternary Derivatives: Effect of the Chain Length of the Oligomers on Complexation. *Polym. J.* **1977,** *9*, 73-78.
- 20. Fu, J.; Schlenoff, J. B., Driving Forces for Oppositely Charged Polyion Association in Aqueous Solutions: Enthalpic, Entropic, but Not Electrostatic. *J. Am. Chem. Soc.* **2016**, *138*, 980-90.
- 21. Jing, B.; Ferreira, M.; Gao, Y.; Wood, C.; Li, R.; Fukuto, M.; Liu, T.; Zhu, Y., Unconventional Complex Coacervation between Neutral Polymer and Inorganic Polyoxometalate in Aqueous Solution via Direct Water Mediation. *Macromolecules* **2019**, *52*, 8275-8284.
- 22. Bosshard, H. R.; Marti, D. N.; Jelesarov, I., Protein Stabilization by Salt Bridges: Concepts, Experimental Approaches and Clarification of Some Misunderstandings. *J. Mol. Recognit.* **2004**, *17*, 1-16.
- 23. Anderson, D. E.; Becktel, W. J.; Dahlquist, F. W., pH-Induced Denaturation of Proteins: A Single Salt Bridge Contributes 3-5 kcal/mol to the Free Energy of Folding of T4 Lysozyme. *Biochemistry* **1990**, *29*,

2403-2408.

- 24. Kumar, S.; Nussinov, R., Close-Range Electrostatic Interactions in Proteins. *ChemBioChem* **2002**, *3*, 604-617.
- Liquid Condensate. *Nat. Rev. Mol. Cell Biol.* **2021**, *22*, 165-182.
- 26. Sanchez de Groot, N.; Armaos, A.; Graña-Montes, R.; Alriquet, M.; Calloni, G.; Vabulas, R. M.; Tartaglia, G. G., RNA Structure Drives Interaction with Proteins. *Nat. Commun.* **2019**, *10*, 3246.
- 27. Perry, S. L.; Leon, L.; Hoffmann, K. Q.; Kade, M. J.; Priftis, D.; Black, K. A.; Wong, D.; Klein, R. A.; Pierce, C. F., 3rd; Margossian, K. O.; Whitmer, J. K.; Qin, J.; de Pablo, J. J.; Tirrell, M., Chirality-Selected Phase Behaviour in Ionic Polypeptide Complexes. *Nat. Commun.* **2015**, *6*, 6052.
- 28. Boulmedais, F.; Ball, V.; Schwinte, P.; Frisch, B.; Schaaf, P.; Voegel, J.-C., Buildup of Exponentially Growing Multilayer Polypeptide Films with Internal Secondary Structure. *Langmuir* **2003**, *19*, 440-445.
- 29. Otis, J. B.; Sharpe, S., Sequence Context and Complex Hofmeister Salt Interactions Dictate Phase Separation Propensity of Resilin-like Polypeptides. *Biomacromolecules* **2022**, *23*, 5225-5238.
- 30. Chen, C.; Wang, Z.; Li, Z., Thermoresponsive Polypeptides from Pegylated Poly-l-glutamates. *Biomacromolecules* **2011**, *12*, 2859-2863.
- 31. Hanski, S.; Junnila, S.; Soininen, A. J.; Ruokolainen, J.; Ikkala, O., Oblique Self-Assemblies and Order–Order Transitions in Polypeptide Complexes with PEGylated Triple-Tail Lipids. *Biomacromolecules* **2010**, *11*, 3440-3447.
- 32. Lee, K.; Noh, Y.; Bae, Y.; Kang, S.; Cha, C., Tunable Physicomechanical and Drug Release Properties of In Situ Forming Thermoresponsive Elastin-like Polypeptide Hydrogels. *Biomacromolecules* **2022**, *23*, 5193–5201.
- 33. Boulmedais, F.; Schwinté, P.; Gergely, C.; Voegel, J. C.; Schaaf, P., Secondary Structure of Polypeptide Multilayer Films: An Example of Locally Ordered Polyelectrolyte Multilayers. *Langmuir* **2002**, *18*, 4523-4525.
- 34. Pilbat, A.-M.; Ball, V.; Schaaf, P.; Voegel, J.-C.; Szalontai, B., Partial Poly(glutamic acid) ↔ Poly(aspartic acid) Exchange in Layer-by-Layer Polyelectrolyte Films. Structural Alterations in the Three-Component Architectures. *Langmuir* **2006**, *22*, 5753-5759.
- 35. Boulmedais, F.; Bozonnet, M.; Schwinté, P.; Voegel, J. C.; Schaaf, P., Multilayered Polypeptide Films: Secondary Structures and Effect of Various Stresses. *Langmuir* **2003**, *19*, 9873-9882.
- 36. Debreczeny, M.; Ball, V.; Boulmedais, F.; Szalontai, B.; Voegel, J.-C.; Schaaf, P., Multilayers Built from Two Component Polyanions and Single Component Polycation Solutions: A Way To Engineer Films with Desired Secondary Structure. *J. Phys. Chem. B* **2003**, *107*, 12734-12739.
- 37. Itoh, K.; Tokumi, S.; Kimura, T.; Nagase, A., Reinvestigation on the Buildup Mechanism of Alternate Multilayers Consisting of Poly(L-glutamic acid) and Poly(L-, D-, and DL-lysines). *Langmuir* **2008**, *24*, 13426-13433.
- 38. Wacławska, M.; Guza, M.; Ścibisz, G.; Fortunka, M.; Dec, R.; Puławski, W.; Dzwolak, W., Reversible Freeze-Induced β-Sheet-to-Disorder Transition in Aggregated Homopolypeptide System. *J. Phys. Chem. B* **2019**, *123*, 9080-9086.
- 39. Fulara, A.; Lakhani, A.; Wójcik, S.; Nieznańska, H.; Keiderling, T. A.; Dzwolak, W., Spiral Superstructures of Amyloid-Like Fibrils of Polyglutamic Acid: An Infrared Absorption and Vibrational Circular Dichroism Study. *J. Phys. Chem. B* **2011**, *115*, 11010-11016.
- 40. Pacalin, N. M.; Leon, L.; Tirrell, M., Directing the Phase Behavior of Polyelectrolyte Complexes Using Chiral Patterned Peptides. *Eur. Phys. J.: Spec. Top.* **2016**, *225*, 1805-1815.
- 41. Cakmak, F. P.; Choi, S.; Meyer, M. O.; Bevilacqua, P. C.; Keating, C. D., Prebiotically-Relevant Low Polyion Multivalency can Improve Functionality of Membraneless Compartments. *Nat. Commun.* **2020**, *11*, 5949.
- 42. Zubay, G.; Wilkins, M. H. F.; Blout, E. R., An X-ray Diffraction Study of a Complex of DNA and a

- Synthetic Polypeptide. J. Mol. Biol. 1962, 4, 69-IN2.
- 43. Haynie, D. T.; Balkundi, S.; Palath, N.; Chakravarthula, K.; Dave, K., Polypeptide Multilayer Films: Role of Molecular Structure and Charge. *Langmuir* **2004**, *20*, 4540-4547.
- 44. Hernik-Magoń, A.; Puławski, W.; Fedorczyk, B.; Tymecka, D.; Misicka, A.; Szymczak, P.; Dzwolak, W., Beware of Cocktails: Chain-Length Bidispersity Triggers Explosive Self-Assembly of Poly-l-Glutamic Acid β2-Fibrils. *Biomacromolecules* **2016**, *17*, 1376-1382.
- 45. Nakashima, K. K.; Baaij, J. F.; Spruijt, E., Reversible Generation of Coacervate Droplets in an Enzymatic Network. *Soft Matter* **2018**, *14*, 361-367.
- 46. Aumiller, W. M.; Keating, C. D., Phosphorylation-Mediated RNA/Peptide Complex Coacervation as a Model for Intracellular Liquid Organelles. *Nat. Chem.* **2016**, *8*, 129-137.
- 47. Greig, J. A.; Nguyen, T. A.; Lee, M.; Holehouse, A. S.; Posey, A. E.; Pappu, R. V.; Jedd, G., Arginine-Enriched Mixed-Charge Domains Provide Cohesion for Nuclear Speckle Condensation. *Mol. Cell* **2020**, *77*, 1237-1250.e4.
- 48. Vondrášek, J.; Mason, P. E.; Heyda, J.; Collins, K. D.; Jungwirth, P., The Molecular Origin of Like-Charge Arginine–Arginine Pairing in Water. *J. Phys. Chem. B* **2009**, *113*, 9041-9045.
- 49. Fisher, R. S.; Elbaum-Garfinkle, S., Tunable Multiphase Dynamics of Arginine and Lysine Liquid Condensates. *Nat. Commun.* **2020**, *11*, 4628.
- 50. Marciel, A. B.; Srivastava, S.; Tirrell, M. V., Structure and Rheology of Polyelectrolyte Complex Coacervates. *Soft Matter* **2018**, *14*, 2454-2464.
- 51. Fonseca, S. B.; Pereira, M. P.; Kelley, S. O., Recent Advances in the Use of Cell-Penetrating Peptides for Medical and Biological Applications. *Adv. Drug Deliv. Rev.* **2009**, *61*, 953-964.
- 52. Fares, H. M.; Ghoussoub, Y. E.; Delgado, J. D.; Fu, J.; Urban, V. S.; Schlenoff, J. B., Scattering Neutrons along the Polyelectrolyte Complex/Coacervate Continuum. *Macromolecules* **2018**, *51*, 4945-4955.
- 53. Sadman, K.; Delgado, D. E.; Won, Y.; Wang, Q.; Gray, K. A.; Shull, K. R., Versatile and High-Throughput Polyelectrolyte Complex Membranes via Phase Inversion. *ACS Appl. Mater. Interfaces* **2019**, *11*, 16018-16026.
- 54. Li, H.; Liu, Y.; Shetty, A.; Larson, R. G., Low-Frequency Elastic Plateau in Linear Viscoelasticity of Polyelectrolyte Coacervates. *J. Rheol.* **2022**, *66*, 1067-1077.
- 55. Harris, J. J.; DeRose, P. M.; Bruening, M. L., Synthesis of Passivating, Nylon-Like Coatings through Cross-Linking of Ultrathin Polyelectrolyte Films. *J. Am. Chem. Soc.* **1999**, *121*, 1978-1979.
- 56. Johnson, C. M., Differential Scanning Calorimetry as a Tool for Protein Folding and Stability. *Arch. Biochem. Biophys.* **2013**, *531*, 100-109.
- 57. Mazurenko, S.; Kunka, A.; Beerens, K.; Johnson, C. M.; Damborsky, J.; Prokop, Z., Exploration of Protein Unfolding by Modelling Calorimetry Data from Reheating. *Sci. Rep.* **2017**, *7*, 16321.
- 58. Sochava, I. V.; Belopolskaya, T. V.; Smirnova, O. I., DSC Study of Reversible and Irreversible Thermal Denaturation of Concertrated Globular Protein Solutions. *Biophys. Chem.* **1985**, *22*, 323-336.
- 59. Blumlein, A.; McManus, J. J., Reversible and Non-Reversible Thermal Denaturation of Lysozyme with Varying pH at Low Ionic Strength. *Biochim. Biophys. Acta Proteins Proteom.* **2013**, *1834*, 2064-2070.
- 60. Arrondo, J. L. R.; Muga, A.; Castresana, J.; Goñi, F. M., Quantitative Studies of the Structure of Proteins in Solution by Fourier-Transform Infrared Spectroscopy. *Prog. Biophys. Mol. Biol.* **1993,** *59*, 23-56.
- 61. Fares, H. M.; Schlenoff, J. B., Equilibrium Overcompensation in Polyelectrolyte Complexes. *Macromolecules* **2017**, *50*, 3968-3978.
- 62. Chen, Y.; Yang, M.; Shaheen, S. A.; Schlenoff, J. B., Influence of Nonstoichiometry on the Viscoelastic Properties of a Polyelectrolyte Complex. *Macromolecules* **2021**, *54*, 7890-7899.
- 63. Mita, K.; Ichimura, S.; Zama, M., Conformation of Poly(L-homoarginine). *Biopolymers* **1980,** *19*, 1123-1135.

- 64. Hammes, G. G.; Schullery, S. E., Structure of Macromolecular Aggregates. I. Aggregation-induced Conformational Changes in Polypeptides. *Biochemistry* **1968**, *7*, 3882-7.
- 65. Terauchi, M.; Tamura, A.; Tonegawa, A.; Yamaguchi, S.; Yoda, T.; Yui, N., Polyelectrolyte Complexes between Polycarboxylates and BMP-2 for Enhancing Osteogenic Differentiation: Effect of Chemical Structure of Polycarboxylates. *Polymers* **2019**, *11*, 1327.
- 66. Quan, B. D.; Wojtas, M.; Sone, E. D., Polyaminoacids in Biomimetic Collagen Mineralization: Roles of Isomerization and Disorder in Polyaspartic and Polyglutamic Acids. *Biomacromolecules* **2021**, *22*, 2996-3004.

For Table of Contents Only

